Latin American Journal of Solids and Structures
www.lajss.org

Thermal load effects on fatigue life of a cracked railway wheel

Abstract

In this paper, fatigue life of a cracked railway wheel under thermo-mechanical loads is studied. For this purpose a FE model of a wheel, with two brake shoes and a portion of rail is created and suitable loads and boundary conditions are applied to the model. It is assumed that the wheel has contained an elliptical crack in the definite depth of the tread surface and thermalloads are determined by modeling the contact of the rail-wheel and two brake blocks. In order to investigate the thermalloads effect on the fatigue life of the cracked wheel, analyses areperformed in two cases: mechanical analysis and thermo-mechanical analysis; while difference between them, shows thermal load effects and its importance. In this work the wheel rotation on rail is modeled and a 3D FE model for determination of rail-wheel contact pressure is used while in many of the previous investigations, either rolling wasn't modeled or its effect was simplified as a translating pressure distribution along the rail-wheel contact region and also the Hertz contact theory had used for determination of contact pressure in wheel- rail interface. Finally, effects of angular velocity on fatigue life of a cracked wheel under -mechanical and mechanical loads are shown. The obtained results confirm the important influences of thermal loads on the wheel fatigue life in all mentioned cases that are studied in this article.

Keywords

Fatigue life; railway wheels; thermo-mechanical loads; crack.

Azadeh Haidari[a]
Parisa Hosseini Tehrani[b*]

[a,b]Center of excellence in railway transportation, School of Railway Engineering, Iran University of Science and Technology, Tehran, Iran
[a]aheidary@rail.iust.ac.ir

Corresponding author:
[b*]hosseini_t@iust.ac.ir

http://dx.doi.org/10.1590/1679-78251658

Received 22.10.2014
In revised form 07.01.2015
Accepted 13.01.2015
Available online 07.02.2015

1 INTRODUCTION

Increasing demands for transporting Commodities and passengers cause a rapid advance in transportation industry and railway vehicles are not excluded from this progress. High speed trains are built and used in many countries; while with any progression in rail vehicles, importance of some problems such as safety and comfort increases. One of the most critical components of railway vehicles are wheels since the wheel failure may result in derailment; therefore an exact design, scrutiny on wheel fatigue problem and knowing effective parameters on their life, can improve the life of whole structure. Because of repeating nature of applied loads to wheels, fatigue damage is a very common damage mechanism which can appears in various modes such as: nucleation and growth of fatigue cracks, spalling, shelling, and so forth. Although the main sources of these

phenomena are rolling contact loads, thermal loads between wheel-rail and wheel-brake block, created in braking stage, presence of structural defects in wheel material and so forth; they may not be omitted in a precise design. What is more increasing of speed aggravates these factors and augmenting the thermal fatigue problem of wheels.

Ekberg and Kabo (2005) present an overview of rolling contact fatigue phenomena occurring at wheels and railsand demonstrate some differences of RCF with classic fatigue analysis. Hossein Tehrani and Saket (2009) studied the fatigue crack initiation life of railroad wheels but effects of thermal and mechanical loads of braking were ignored and rolling of wheel was not modeled. Haidari and Hosseini Tehrani (2014) researched on the fatigue of railway wheels under combined thermal and mechanical loads but in their paper the crack was not modeled and fracture life of wheel wasn't studied. Considering the high importance of service loads on the fatigue occurrence in wheels, it is necessary to mention all loads applied to the wheel, such as, in addition to mechanical loads, thermal loads created at braking stage should be considered (Chuanxi et al. 2009; Wanming et al., 2009); in other words, for obtaining a reliable life of crack propagation in a railway wheel and prediction of cracked wheel behavior under service loads, a thermo- mechanical analysis should be performed. For a wheel with a very shallow crack, effect of combined thermal and mechanical loads on the growth of existing crack is very significant (Huang and Ju 1985). Therefore, for a precise fatigue analysis, effects of both thermal and mechanical loads should be considered. Some recent researches on the braking thermal stresses and crack analysis and assumptions used are as follow:

Guagliano and Vergani (2005), used a semi-analytical approach for analysis of internal cracks in railway wheels. Lansler and Kabo (2005), proposed a 2D FE model to get the face displacement of internal cracks in wheels. Liu et al. (2007) using the computational finite element method, calculated the history of stress intensity factor of the 3D rail- wheel contact stress. Feng et al. (2006) studied the growth behavior of subsurface cracks under different load paths and concluded that the models based on strain energy release rate cannot embrace this effect and a mixed mode crack growth model is necessary. Yevtushenko and Kuciej (2010) proposed an analytical solution for determination of temperature and thermal stresses in the pad- disc contact area and thermal cracks in this region is studied by Mackin et al. (2002). Gallardo-Hernandez et al. (2006) used the twin- disc test approach for studying abrasion and rolling contact fatigue of wheels and obtained temperature of each disc (which are corresponding to rail and wheel) by a thermocamera.

Peng et al. (2012) provided a prediction of the crack growth due to cyclic braking loads, mechanical loads and residual stresses due to manufacturing process in the railway wheels. They used a 3D non-linear FE model to calculate thermal stress of the wheel; but in their work, blocks were not been modeled and average brake power was applied to the tread region of the wheel uniformly, therefore effects of local heating of wheel were not considered.

In despite of relatively high number of works done on the fatigue problem of railway wheels, combined effects of thermal and mechanical loads in a cracked wheel is rarely investigated and in the most of existing papers, some assumption are considered which reduce reliability and accuracy of obtained results.

In this paper, it is tried to improve the previous works by the means of modeling rail and brake blocks instead of using assumptions about effects of these parts and their applied loads to the

wheel. Besides, wheel rotation on the rail is modeled and a 3D FE model for determination of rail-wheel contact pressure is used, while in many of the previous investigations, either rolling isn't modeled or its effect is simplified as a translating pressure distribution along the rail-wheel contact region and the Hertz contact theory is used for determination of contact pressure in wheel- rail interface.

2 FE ANALYSIS OF RAIL, WHEEL AND BRAKE BLOCKS

2.1 Thermal and mechanical loads

Rolling contact loads in the rail-wheel contact region, however, create the greatest mechanical stress fields; other mechanical loads such as friction force between rail and wheel, brake pressure and so forth affect mechanical stress fields of the wheel. In many of previous works, effects of these forces were ignored; but in this article, for having the reliable model, the shear stresses due to rail-wheel friction force are considered. In addition, as another mechanical load, the brake pressure which compresses the brake shoes to the wheel tread surface in braking stage is considered. Thermal loads created in braking step also are applied to the model in order to obtain the most accurate responses and as mentioned previously, instead of Hertzian contact theory, a 3D FE method is used for modeling of rail- wheel contact process.

2.2 Thermal and mechanical analysis

To get the thermal stress fields, the temperature rise due to braking should be obtained and for this reason, it is assumed that the whole of frictional energy created at wheel-blocks contact area (brake power) converts to heat and this heat, distributes among rail, wheel and brake blocks proportional to their conductivity, initial temperature, heated area and so forth. Hence for determining temperature rise of these components; it is necessary to define a parameter as the heat partition factor, which describes what portion of heat generated in contact region of two bodies, is transferred to each of them. This quantity in the rail-wheel and wheel-block contact area, is defined by α and β, respectively (α and β are representatives of fraction of generated heat transferred to the wheel). The analytical analysis of heat partition factors are derived assuming one-dimensional heat conduction in the bodies that the two bodies have equal temperature at contact. Analytical calculation for heat partitioning can be found in Vernersson (2007). At the beginning of Wheel sliding on the rail, heat partition factor between rail and wheel (α) is equal to 0.5; this is due to considering the same physical and thermal properties for the wheel and rail. By increasing the slip time, this factor reduces, which means that the most of heat generated due to slip is transferred to rail.

The reason for this reduction can be basedon the fact that during rotation of the wheel on the rail, a new rail surface is always subjected to the high temperature wheel Surface; therefore the rail surface should absorb this generated heat until attained to the wheel temperature. As mentioned, in the beginning of sliding, α is equal to 0.5 (transient state) and after some times it reaches a constant value (steady state). In this task, transient termal analysis is done, and $\alpha = 0.5$ is applied to the model.

For the wheel-block contact, the following equation may be used to determine "β".

$$\beta = \left[1 + \left(\frac{k_w}{k_b}\right)^{1/2} \frac{K_b}{K_w}\frac{A_b}{A_w}\right]^{-1} \tag{1}$$

In which A_w and A_b are the areas which are swept by the contact (A_w is the wheel circumference multiplied by the block width). The length and width of blocks are considered 250 and 100 mm respectively. Thermal parameters used for wheel, rail and blocks are as follows:

$k_{r,w} = 11.8{*}10^{-6}$ ($m^2/^oC$), $C_{pr,w} = 540$ (J/Kg^oC), $K_{r,w} = 50$ (W/m^oC), $a_{r,w} = 2{*}10^{-5}$ ($1/K$)

$k_b = 11.7{*}10^{-6}$ ($m^2/^oC$), $C_{pb} = 480$ (J/Kg^oC), $K_b = 40$ (W/m^oC), $a_b = 1.2{*}10^{-6}$ ($1/K$)

Which r, w and b are the symbols for rail, wheel and block respectively also C_p, k, a, and K refer to specific heat, thermal diffusivity, thermal expansion and coefficient of thermal conductivity respectively. Here the value of β according to mechanical and thermal properties of blocks and wheel is approximately equal to 0.9 (Vernersson, 2007).

These mensioned heat partition factors are used to model the contact of rail-wheel and wheel-block in Abaqus software.

In this article, unlike the most previous researches done for determining temperature rise due to braking, the effect of convectional cooling is considered which due to rotation of wheel and high speed of air flow around it, convection factor of $h = 100$ $W/m^{2o}C$ is considered. As had indicated by Ramanan et al. (1999), temperature-independent material model does not change the results appreciably in comparison to temperature-dependent material model and hence the first model (the temperature independent model) is used.

The brake block configuration used in this article is: $2Bg$ (two blocks per two holders) and is shown in Figure 1.

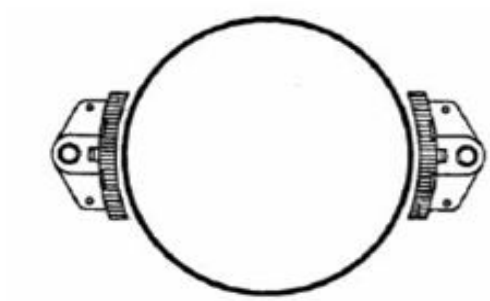

Figure 1: Blocks arrangement used in this paper.

2.3 Fatigue crack growth life prediction

Based on Association of American Railroad (AAR) investigation on the three types of railway wheels used in passenger trains, the rate of initiation and growth of thermal cracks in these

wheels is very high and the rail-wheel contact band is exposed to the higher possibility of thermal cracks initiation compared with the other areas (Grundy 1994). Fracture toughness (K_{IC}) which is a parameter describes resistance of a material against the unstable crack growth, may be obtained by test and used for determination of critical crack size (a_c) in wheel. From existing field observations, subsurface crack in wheel, usually occurs at depth of 5–10 mm with about 20^{o} inclination. On the other hand, based on experimental observations and also temperature fields obtained from the presented FE model, the thermal loads of braking only are limited to a narrow layer of tread surface and by increasing the depth, the importance of thermal stress fields reduces and in the depth of 6% of wheel diameter, thermal load effects can be neglected (Tudor and Khonsari, 2006). Therefore the most critical case for a cracked railway wheel, occurs when the crack has a small depth so that the both mechanical and thermal stress, affect growth of it. In the current study, the subsurface crack is assumed to be 6 mm below the tread surface with an inclination angle of 20^{o}. As it is shown in Figure 2, the 20^{o} inclination is the angle between the minor axis of the crack and the YZ-plane. The wheel model used in this article, contained an elliptical crack with semi-axis length of $a = 5$ mm and $b = 7.5$ mm, which is embedded in a plane with 20 degrees inclination with horizontal plane (parallel to the wheel- rail contact plane) in depth of 6 mm from tread surface.The vertical load applied on the wheel is assumed to be the maximum design load, which is considered equal to 146.2 kN.

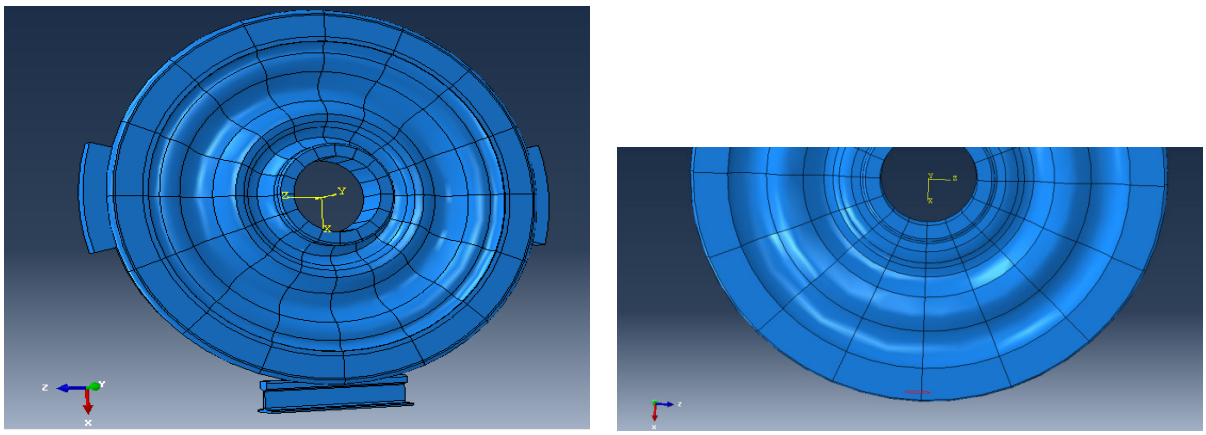

(a) (b)

Figure 2: (a) Finite element model of rail, wheel and brake blocks. (b) Crack location.

The wheel boundary conditions, as it is shown in Figure 2, is free rotation about "y" axis with angular velocity of 50 rad/s and translations along the "x" axis. Other movments are considered to be fixed. All of these BCs are applied to a reference point considered at the wheel center where the axle load is applied. The element type used in this paper for all parts (rail, Wheel and brake shoes) is an 8-node thermally coupled brick, trilinear displacement and temperature (C3D8T). Besides a contour-integral based method which is readily available in Abaqus is used for crack modeling and to produce a square root singularity of stress field, singular (quarter point) elements are used in the first ring of elements surrounding the crack front. Used database model is Standard/Explicit Model and Standard Server Benchmarks.

Since crack propagation is controlled by the stress field near the crack tip, accurate calculation of tress intensity factor plays an essential role in fracture mechanics. In this paper the stress intensity factor is evaluated directly based on displacement discontinuities using a three-dimensional finite element model. By knowing the crack tip element displacements, for fixed crack dimensions, the Mode I, Mode II and Mode III stress intensity factors (KI, KII and KIII) can be directly calculated using Equations 2, 3 and 4 (Sheibani and Olson, 2013).

$$K_I = C\frac{D_n E\sqrt{\pi}}{4\left(1-\nu^2\right)\sqrt{P}} \tag{2}$$

$$K_{II} = C\frac{D_s E\sqrt{\pi}}{4\left(1-\nu^2\right)\sqrt{P}} \tag{3}$$

$$K_{III} = C\frac{D_t E\sqrt{\pi}}{4\left(1+\nu\right)\sqrt{P}} \tag{4}$$

Where"E" is modulus of elasticity, "ν" is Poisson's ratio, "P" is crack tip element length perpendicular to crack front, "D_n" is the opening displacement discontinuity of crack tip element, "D_s" is shear displacement discontinuity perpendicular to "D_n" and the crack front, "D_t" is front-parallel displacement discontinuity (Figure 3) and "C" is an empirically determined constant that accounts for the discrepancy between the numerical approximation and the analytical solution. In this paper $C = 0.806$ is used (Sheibani and Olson, 2013).

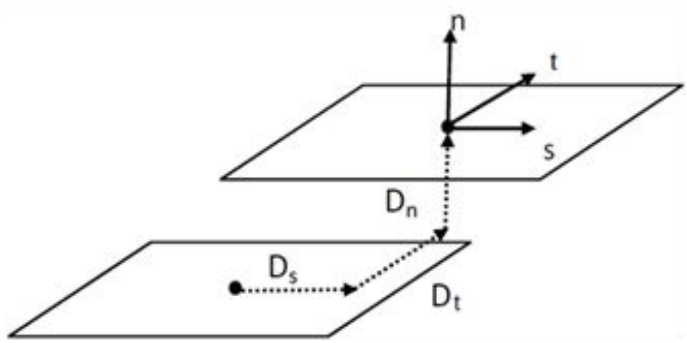

Figure 3: Displacement discontinuity modeling.

Liu et al. (2007) developed a mixed-mode fatigue crack threshold criterion considering multiaxial fatigue limit criteria and the Kitagawa–Takahashi diagram. According to Liu et al., the mixed-mode fatigue crack threshold criterion may be used for fatigue crack propagation analysis. They expressed the general crack propagation as equation (5).

$$K_{mixed,eq} = \frac{1}{B}\sqrt{K_I^2 + \left(\frac{K_{II}}{s}\right)^2 + \left(\frac{K_{III}}{s}\right)^2 + A\left(\frac{K^H}{s}\right)^2} \tag{5}$$

In this equation, material parameter "s" is related to the material ductility and effects of the critical plane orientation and describes as the ratio of mode II and mode I stress intensity factors under a specific crack growth rate. In this work the amount of "s" for railway wheel is assumed to be 0.6. The superscript "H" indicates the hydrostatic stress related term. "A" and "B" are material parameters that are listed in Table 1.

Material property	$s \le 1$	$s > 1$
γ	$\cos(2\gamma) = \dfrac{-2 + \sqrt{4 - 4\left(1/s^2 - 3\right)\left(5 - 1/s^2 - 4s^2\right)}}{2\left(5 - 1/s^2 - 4s^2\right)}$	$\gamma = 0$
A	$A = 0$	$A = 9\left(s^2 - 1\right)$
B	$B = \left[\cos^2(2\gamma)s^2 + \sin^2(2\gamma)\right]^{1/2}$	$B = s$

Table 1: Material parameters for fatigue crack propagation prediction (Liu et al., 2007)

After determination of critical crack size (a_c) and stress intensity factors for modes I, II and III, The general crack propagation function may be expressed as:

$$\frac{\mathrm{d}a}{\mathrm{d}N} = C\left[\frac{\Delta K_{eff}}{\left(1-R\right)^{\zeta}}\right]^{m} \tag{6}$$

Where $\mathrm{d}a/\mathrm{d}N$ is the crack growth rate, ΔK_{eff} is the effective stress intensity factor range for mixed-mode loading, R is the stress ratio and finally C, m and ζ are material parameters. For the data reported by Kuna et al. (2005), C, m and ζ are determined byregression analysis as $5.8*10^{-9}$, 2.95 and 1, respectively. The subsurface crack propagation studied in this paper is shear dominated (mode II and mode III) because the normal stress is compressive and therefore crack growth doesn't occur in mode I. The mode II and III stress intensity factors (SIF) histories of crack tip at the major axis (points 1 in Figure 4) during one revolution of the wheel for the initial crack lengths ($a = 5$ mm, $b = 7.5$ mm) are obtained from mechanical and thermo-mechanical analyses and are shown in Figure 5. In Figure 6 the stress intensity factor values of presented

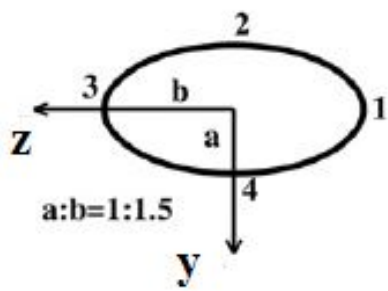

Figure 4: Points considered on the crack surface for stress intensity factor calculation.

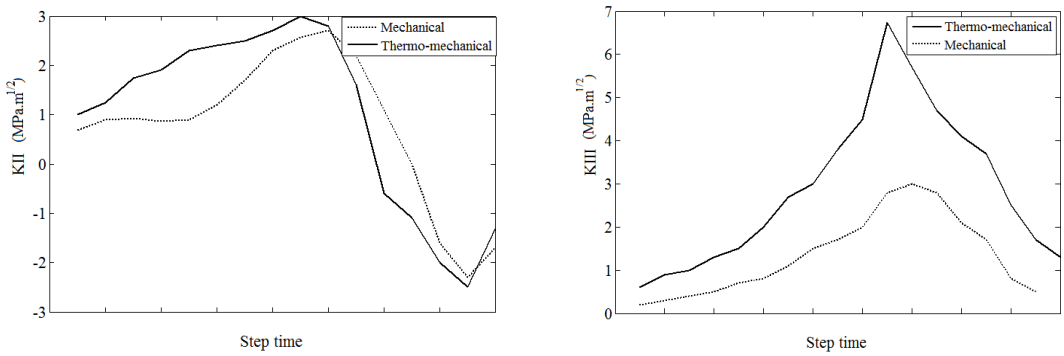

Figure 5: Stress intensity factor history of point "1" (In Figure 4) under mechanical and thermo-mechanical analyses.

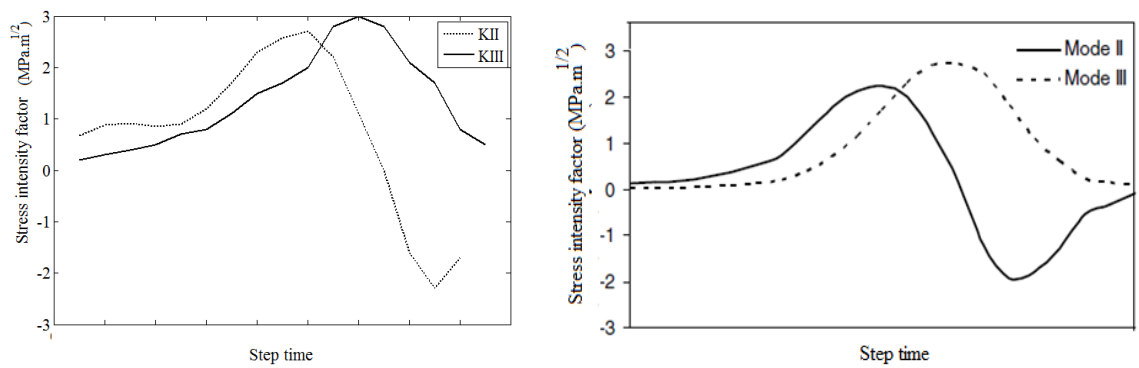

(a) (b)

Figure 6: (a) Stress intensity factor history of presented mechanical analysis. (b) Stress intensity factor history of rolling contact analysis by Liu et al. (2007).

mechanical analysis are compared to results of Liu et al. (2007) and an acceptable accordance may be seen. In presented mixed-mode crack growth mode, all SIFs for different modes are combined using equation (5), while calculated equivalent SIF may be correlated to material's mode I crack growth curve for life prediction. For mode II and mode III SIFs, their stress ratio is either 0 or a finite negative value close to -1 depending on their locations Thus, the stress ratio of transformed equivalent SIF is also in the range of 0 and a finite negative value. In this paper this parameter is close to 0 and therefore $R=0$ is applied in equation (6).

Equation (6) can be written as a separable statement and the number of required cycles for initial crack in wheel to attain the critical size may be obtained as:

$$N(a)=\frac{1}{C(\Delta F)^m}\int_{a_0}^{a_c}\frac{(1-R)^{\zeta m}\,\mathrm{d}a}{\left[\sqrt{\pi a}Y(a)\right]^m} \tag{7}$$

Where ΔF is the applied vertical loading range and $Y(a)$ is a geometry function considering the effect of crack configuration and boundary conditions, that is calculated using the finite element results through incremental crack growth. In this work, the considered value of K_{IC} for railway wheel is 85 $\mathrm{MPa}\sqrt{\mathrm{m}}$ (Strnadel and Hausild, 2008).

3 RESULTS AND DISCUSSION

3.1 Finite Element Model of Wheel – Rail – Brake blocks system

To built a realistic model and obtain the more accurate stress fields of wheel, a 3D elasto-plastic finite element model is used. This model should be able to accurately calculate the 3D state of stresses in the contact region of rail-wheel and wheel-blocks as well as includes material nonlinearity. In this research, Abaqus 6.10 is used for these purposes.

To obtain the mechanical stress fields and also thermal stresses created at braking stage, two cast iron brake blocks and a wheel, which rotates on a portion of a rail with length of 600mm, are modeled. The length of modeled rail is equal to distance between two sleepers and boundary conditions at its cutting edges are fixed. Previous studies on the mechanical loads of railway wheels, show that nucleation and growth of cracks (sub-surface cracks) often occur in the depth of 5-10 mm. On the other hand, based on experimental observations and also temperature fields obtained from presented FE model, the thermal loads of braking are limited to a narrow layer of tread surface and by increasing the depth, the importance of thermal stress fields reduces and in the depth of 6% of wheel diameter, thermal load effects may be neglected (Tudor and Khonsari, 2006). Therefore the most critical case for a cracked railway wheel, occurs when the crack has a small depth so that the both mechanical and thermal stress, may affect its growth. In this study it is assumed that the wheel contained an elliptical crack in the depth of 6mm from tread surface with semi-axis equal to $a = 5$ mm, and $b = 7.5$ mm.

Two steps are used in this analysis: rotation and braking steps. Axle load, rail- wheel contact and rotation of wheel is defined in the rotation step, while in braking step which is defined after rotation step, the brake pressure of 0.7 MPa is applied to each of brake blocks and compress them to the tread surface of the wheel.

Interactions between rail-wheel and brake blocks-wheel is considered as surface to surface contact in Abaqus and in both interactions, the wheel surface is considered as the master surface while the rail and brake blocks surfaces are assumed as the slave surfaces. The rail-wheel interaction is applied at the both rotation and braking steps and the wheel-brake blocks interaction is only applied to the braking step. The friction formulation used is penalty with friction coefficient of 0.3 between rail-wheel and 0.15 between wheel-brake blocks. The normal behavior is considered as "hard contact" and thermal conductance in rail-wheel contact and wheel-blocks contact are 50 and 40 (W/m^oC) respectively. The heat partition factors are applied as the fraction of converted heat distributed to slave and master surfaces. For considering the convection effects, a surface film condition interaction is considered for the wheel surface with the film coefficient of 100 (convection factor) in the Abaqus model.

Consideration of both thermal and mechanical loads, necessitates that all elements of model possess both thermal and mechanical DOF and therefore, they are meshed with coupled temperature-displacement elements (C3D8T elements). Due to modeling the wheel rotation, the contact region of wheel is not fixed and thus it is necessary to use relatively fine mesh with equal element size at tread surface of wheel.

A pilot node is considered at the center of wheel that the axle load and all of wheel boundary conditions are applied to this point.

The nominal axle load of 146.2 kN has been considered as the vertical load in this paper. This vertical load transferred to the wheel through axle. The brake pressure is applied to the brake shoes and this pressure via the contact between brake blocks and tread, transmits to the wheel tread and therefore in addition to axle load, the brake power is applied to the wheel tread surface. On the other hand by defining the friction coefficient and slip between rail and wheel, in addition to vertical load, the horizontal loads insert to the wheel tread surface. Generally the stresses experienced by the railway wheel during service are due to vertical axle load, slip and friction forces and thermal braking loads, that all are included in the present study.

The angular velocity of wheel is considered to be 50 rad/s and the material properties of the rail and wheel are assumed to be the same and as follow: Young's modulus 210 MPa, Poisson's ratio 0.3 and rail- wheel friction coefficient 0.3. The linear isotropic hardening model is used in this study. Mechanical and thermal properties of brake blocks are adopted correspond to cast iron blocks and the wheel is made of steel grade R7T with hardness properties that is mentioned in Table 2 (Bernasconi et al., 2005):

Plastic stress (MPa)	Plastic strain
545	0
763.625	0.02099
887.25	0.0445
958.125	0.0863

Table 2: Linear isotropic hardening properties of steel R7T.

3.2 Temperature field

During tread braking process the heat generated by frictional forces is distributed either as severe thermal gradients within the near surface or more gradually over the wheel rim and plate, depending on the intensity of the heating source. Block braking of a wagon or a locomotive is performed by pressing the brake block(s) against the tread of the rotating wheel, which also is in rolling contact with the rail (Peng et al., 2013). In this paper using the rail and brake block modeling, temperature rise due to braking is obtained. In order to account for the dissipation of the thermal heat to the surroundings, a convectional boundary condition is applied to the surface of the wheel. As the wheel rotates, the tread surface is subjected to periodic heating and cooling. The temperature field of tread surface is shown in Figure 7.

To clarify important effects of braking thermal loads on the stress fields and fatigue life of a cracked wheel, results of thermo-mechanical analysis compared to pure mechanical stress responses of the wheel. For this reason, the calculations of critical crack size (a_c), stress intensity factors (SIFs) and equivalent stress intensity factor range (ΔK_{eq}), at one stage by considering thermal loads of braking and at the other stage, without considering these thermal loads are obtained. The relatively large difference between results of these two cases, make clear the importance of thermal stresses and shows that ignoring them, get inaccurate and non-conservative results for fatigue life estimation of wheels under considered loading cycles. The obtained crack growth pattern for mechanical and thermo-mechanical analyses are shown in Figure 8. It may be seen that the numerical prediction of the crack shape agrees well with the field observation.

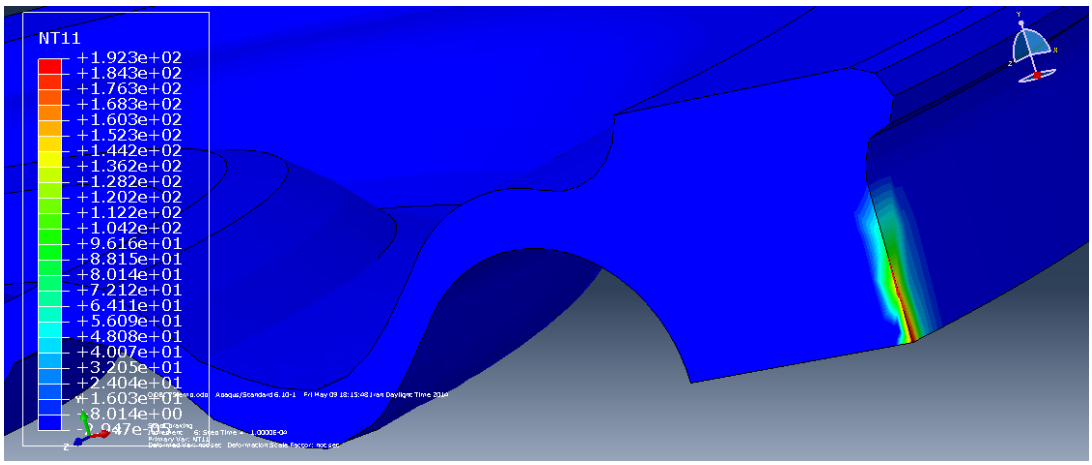

Figure 7: Temperature profile in wheel.

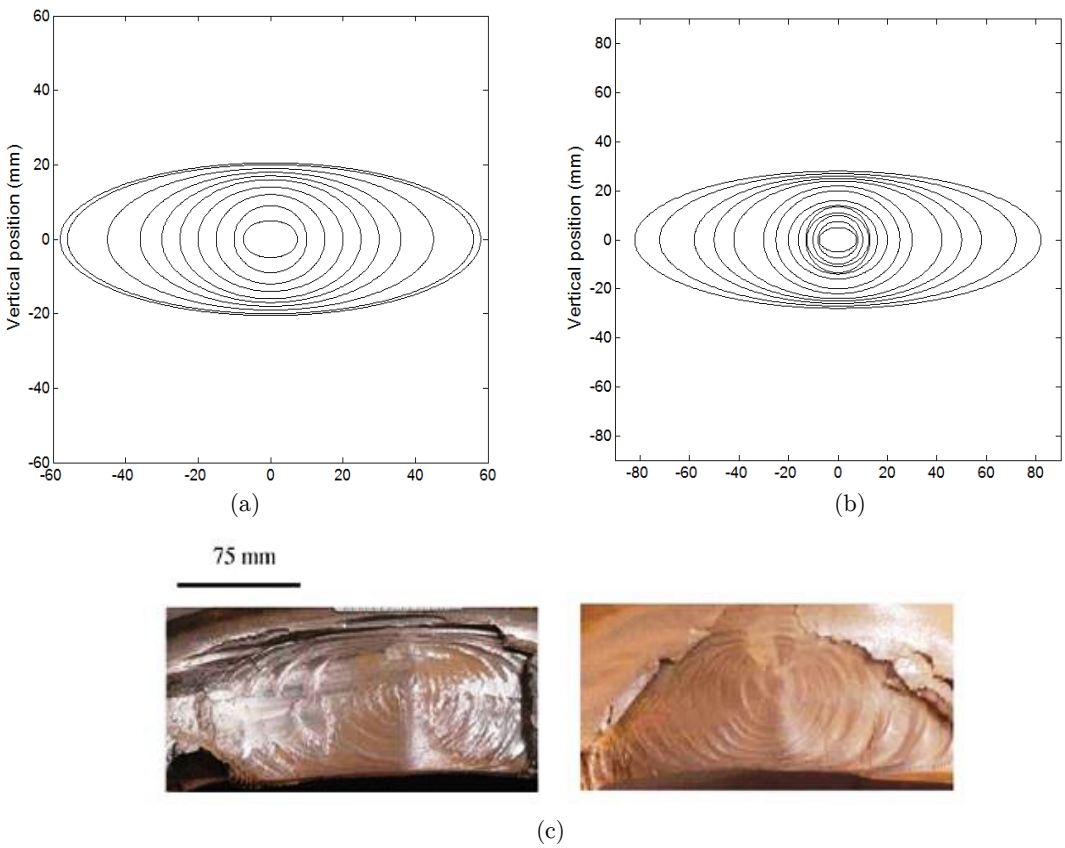

Figure 8: Numerical crack shape obtained from FE analysis of rail-wheel-brake block system: (a) Thermo-mechanical analysis. (b) Mechanical analysis. (c) Field observations of crack shape.

In the early stages, the crack propagation is in an approximately circular configuration, which shows almost equal crack propagation in both minor and major axis directions. Then the crack propagates in an elliptical manner, which is mainly along the major axis direction (track direction).

In Table 3, the obtained results of mechanical and thermo-mechanical critical crack length and fatigue life of the considered cracked railway wheel rotating at angular velocity of 50 rad/s is shown.

	Thermo-mechanical analysis	Mechanical analysis
Critical crack length (a_c)	58 m	82 mm
Fatigue life (10^6 cycles)	1.4	0.9

Table 3: Difference between mechanical and thermo-mechanical analysis of the cracked wheel in angular velocity of 50 rad/s.

Comparison of critical crack sizes of this table shows that with the same initial crack size, fatigue life to crack propagation under thermo-mechanical stress fields is smaller in comparison of the same wheel under only mechanical stress fields. As a result it may be concluded that thermal loads and resultant thermal stresses of braking may have an important role in reduction of fatigue life of cracked wheels, through increasing stress intensity factor range and reducing the critical crack size.

To study the effects of velocity on temperature rise and stress intensity factor, three angular velocities: 50, 75 and 100 rad/s is examined. The results obtained from this study show that the temperature field of wheel is very sensitive to velocity and an increase of this parameter, leads to a high increase of wheel temperature. On the other hand, both mechanical and thermo-mechanical stress fields of wheel augment due to increase of wheel velocity and therefore at higher velocities, the greaterstress intensity factor components are obtained and therefore, life of wheel reduces. Effects of velocity on the stress intensity factors and temperature of wheel for mentioned velocities are listed in Table 4. The SIF values of this table are computed for the initial crack lengths ($a = 5$ mm, $b = 7.5$ mm). As can be seen from data of this table, equivalent stress intensity factor obtained from thermo-mechanical analysis is considerably greater than the corresponding value of mechanical analysis which means that the stresses of crack tip may be increased due to thermal loads of braking.Also, from this table, it may be concluded that an increase of velocity causes the greater values of SIFs and have a destructive effect on the fatigue life of a cracked railway wheel.

	50 rad/s	75 rad/s	100 rad/s
Thermo-mechanical KII ($\mathrm{MPa}\sqrt{\mathrm{m}}$)	3.252	5.93	7.96
Mechanical KII ($\mathrm{MPa}\sqrt{\mathrm{m}}$)	2.71	4.51	6.01
Thermo-mechanical KIII ($\mathrm{MPa}\sqrt{\mathrm{m}}$)	4.451	9.94	13.87
Mechanical KIII ($\mathrm{MPa}\sqrt{\mathrm{m}}$)	3.00	7.14	9.6
Thermo-mechanical $K_{mixed-eq}$ ($\mathrm{MPa}\sqrt{\mathrm{m}}$)	9.187	19.291	26.653
Mechanical $K_{mixed-eq}$ ($\mathrm{MPa}\sqrt{\mathrm{m}}$)	6.73	14.033	18.877
Maximum temperature (^{o}C)	192.3	320.4	424.5

Table 4: Effect of velocity on the mechanical and thermo-mechanical analyses.

Temperatures indicated in Table 4 are representative of the maximum temperature of tread wheel during the braking step analysis. For the angular velocity of 100 rad/s, the result obtained from Abaqus thermal analysis is 424.5 ^{o}C which is analogical to the thermal image generated by thermo camera in a brake rig experiment (Vernersson and Lunden, 2007). Also according to Fec (1985) tread surface can reach temperature of 300-400 ^{o}C.

4 CONCLUSION

In this article, fatigue life of a cracked railway wheel under mechanical loads (rolling contact loads, friction forces and brake pressure) and thermal loads (thermal stresses due to temperature rise during braking) using Abaqus software, has been studied and the following results are obtained:

1- The differences between mechanical stresses (and their resultant fatigue life) and thermo-mechanical stress fields (and their corresponding fatigue crack growth life) demonstrate the non-negligible effect of thermal loads in fatigue investigation of cracked railway wheels.
2- To obtain the reliable results for fatigue life of cracked wheels, braking thermal loads should be considered in the best way and for this reason, the use of 3D FEM, because of considering the local effects of thermal loads that create high stresses and other advantages stated in this article, seems to be one of the best approaches that may be used.
3- Neglecting the effect of braking thermal loads, causes the estimated wheel fatigue crack growth life to be higher than its real value; therefore a non-conservative life prediction may be obtained.
4- Comparing the results of Table 4 for three angular velocities of 50, 75 and 100 rad/s, shows that as the velocity increases, difference between equivalent stress intensity factor from mechanical and thermo-mechanical analyses increases too, so that in angular velocity of 50 rad/s, this difference is about 36%, while in 75 and 100 rad/s, differences between obtained mechanical and thermo-mechanical equivalent stress intensity factor are 37% and 41%, respectively, which imply on this reality that at higher velocities, importance of thermal loads on the fatigue life of the cracked railway wheels, increase and neglecting these thermal loads may lead to a low safety factor of wheel design and also the high possibility of catastrophic failure.

The general results of this paper, reveal the necessity of exact modeling of thermal and mechanical loads, in order to perform an exact thermo-mechanical analysis of railway wheels to achieve the most accurate and reliable results.

References

Bernasconi, A., Davoli, P., Foletti, S., (2005). Comportamento a fatico in stato di sollecitizione multiassial di un acciaio per ruote ferroviarie. Associazione Italiana Per L'Analysi Delle Sollecitazioni, XXXIV CONVEGNO NAZIONALE, Politecnico di Milano, Via La Masa 34 (20158) Milano, Italia, 14–17 SETTEMBRE.

Chuanxi, S., Jun, Z., Chunyan, W., Xueshan, Z., (2009). Thermo-Contact Coupling Finite Element Method Analysis of Wheel/rail Under Sliding Status. International Conference on Information Engineering and Computer Science (ICIECS), Wuhan, INSPEC Accession Number: 11032803.

Ekberg, A., Kabo, E., (2005). Fatigue of railway wheels and rails under rolling contact and thermal loading—an overview. Wear 258: 1288–1300.

Fec, M.C., (1985). Thermal-mechanical damage in railroad wheels due to hot. Wear 102: 31–42.

Feng, M., Ding, F., Jiang, Y., (2006). A study of loading path influence on fatigue crack growth under combined loading. International Journal of Fatigue 28: 19–27.

Gallardo-Hernandez, E.A., Lewis, R., Dwyer-Joyce, R.S., (2006). Temperature in a twin-disc wheel/rail contact simulation. Tribology International 39: 1653–1663.

Grundy, D.C., (1994). Fatigue and fracture of railway wheel steel. Thesis (M.S.) Massachusetts Institute of Technology, Deptartment of Materials Science and Engineering.

Guagliano, M., Vergani, L., (2005). Experimental and numerical analysis of sub-surface cracks in railway wheels. Engineering Fracture Mechanics 72: 255–269.

Haidari, A., Hosseini Tehrani, P., (2014). Fatigue analysis of Railway wheels under combined thermal and mechanical loads. Journal of Thermal Stresses 37: 34–50.

Hosseini Tehrani, P., Saket, M., (2009). Fatigue crack initiation life prediction of railroad. Journal of Physics: Conference series Vol 181.

Huang, J.H., Ju, F.D., (1985). Themomechanical cracking due to moving frictional loads. Wear 102: 81–104.

Kuna, M., Springmann, M., Ma¨dler, K., Hu¨bner, P., Pusch, G., (2005). Fracture mechanics based design of a railway wheel made of austempered ductile iron. Engineering Fracture Mechanics 72: 241–53.

Lansler, E., Kabo, E., (2005). Subsurface crack face displacements in railway wheels. Wear 258: 1038–1047.

Liu, Y., Liu, L., Mahadevan, S., (2007). Analysis of subsurface crack propagation under rolling contact loading in railroad wheels using FEM. Engineering Fracture Mechanics 74: 2659-2674.

Mackin, T.J., Noe, S.C., Ball, K.J., Bedell, B.C., Bim-Merle, D.P., Bingaman, M.C., Bomleny, D.M., Chemlir, G.J., Clayton, D.B., Evans, H.A., Gau, R., Hart, J.L., Karney, J.S., Kiple, B.P., Kaluga, R.C., Kung, P., Law, A.K., Lim, D., Merema, R.C., Miller, B.M., Miller, T.R., Nielson, T.J., O'Shea, T.M., Olson, M.T., Padilla, H.A., Penner, B.W., Penny, C., Peterson, R.P., Polidoro, V.C., Raghu, A., Resor, B.R., Robinson, B.J., Schambach, D., Snyder, B.D., Tom, E., Tschantz, R.R., Walker, B.M., Wasielewski, K.E., Webb, T.R., Wise, S.A., Yang, R.S., Zimmerman, R.S., (2002). Thermal cracking in disc brakes. Engineering Failure Analysis 9: 63-76.

Peng, D., Jones, R., Constable, T., (2013). An investigation of the influence of rail chill on crack growth in a railway wheel due to braking loads. Engineering Fracture Mechanics 98: 1–14.

Peng, D., Jones, R., Constable, T., Lingamanaik, S.N., Chen, B.K., (2012). The tool for assessing the damage tolerance of railway wheel under service conditions. Theoretical and Applied Fracture Mechanics 57: 1-13.

Ramanan, L., Kumar, R.K., Sriraman, R., (1999). Thermo-Mechanical finite element of a rail wheel. International journal of mechanical sciences 41: 487-505.

Sheibani, F., Olson J., (2013). Effective and Sustainable hydraulic fracturing (ed). Chapter 37: Stress Intensity Factor Determination for Three-Dimensional Crack Using the Displacement Discontinuity Method with Applications to Hydraulic Fracture Height Growth and Non Planar Propagation Paths, ISBN 978-953-51-1137-5.

Strnadel, B., Hausild, P., (2008). Statistical scatter in the fracture toughness and Charpy impact energy of pearlitic steel. Material science and engineering 486: 208-214.

Tudor, A., Khonsari, M.M., (2006). Analysis of Heat Partitioning in Wheel/Rail and Wheel/Brake Shoe Friction Contact: An Analytical Approach. Tribology Transactions 49: 635-642.

Vernersson, T., (2007). Temperatures at railway tread braking. Part 1: modeling. J. Rail and Rapid Transit 221: 167-182.

Vernersson, T., Lunden, R., (2007). Temperatures at railway tread braking. Part 3: wheel and block temperatures and the influence of rail chill. Proc. IMechE Vol. 221 Part F: J. Rail and Rapid Transit.

Wanming, Q., Jun, Z., Chuanxi, S., Shengwu, W., (2009). Finite element analysis of wheel-rail thermal-contact coupling when the wheel's sliding. International Conference on Information Engineering and Computer Science (ICIECS), Wuhan, INSPEC Accession Number: 11032950.

Yevtushenko, A., Kuciej, M., (2010). Temperature and thermal stresses in a pad/disc during braking. Applied Thermal Engineering 30: 354-359.